Acta Crystallographica Section D
Biological Crystallography
ISSN 0907-4449

Crystallization and preliminary X-ray diffraction study of the farnesyl diphosphate synthase from *Trypanosoma brucei*

Junhong Mao,[a] Yi-Gui Gao,[b] Sarah Odeh,[a] Howard Robinson,[c] Andrea Montalvetti,[d] Roberto Docampo[d] and Eric Oldfield[a]*

[a]Department of Chemistry, University of Illinois at Urbana-Champaign, 600 South Mathews Avenue, Urbana, Illinois 61801, USA, [b]School of Chemical Sciences, University of Illinois at Urbana-Champaign, 600 South Mathews Avenue, Urbana, Illinois 61801, USA, [c]Department of Biology, Brookhaven National Laboratory, Upton, NY 11973, USA, and [d]Department of Pathobiology and Center for Zoonoses Research, University of Illinois at Urbana-Champaign, 2001 South Lincoln Avenue, Urbana, Illinois 61802, USA

Correspondence e-mail: eo@chad.scs.uiuc.edu

Received 6 July 2004
Accepted 20 August 2004

Farnesyl diphosphate synthase (FPPS) catalyses the formation of farnesyl diphosphate from dimethylallyl diphosphate and isopentenyl diphosphate and is an RNAi-validated drug target in *Trypanosoma brucei*, the causative agent of African sleeping sickness. A *T. brucei* FPPS (390 amino acids) has been expressed in *Escherichia coli* and the recombinant protein has been crystallized in the absence and presence of the bisphosphonate inhibitor minodronate. Diffraction data were collected at 100 K using synchrotron radiation from both crystal types. Crystals obtained in the absence of minodronate belong to space group *I*222, with unit-cell parameters a = 61.43, b = 118.12, c = 120.04 Å, while crystals grown in the presence of minodronate belong to space group *C*2, with unit-cell parameters a = 131.98, b = 118.10, c = 63.25 Å, β = 112.48°. An initial model of the drug-free protein has been built using a homology model with the molecular-replacement method and refined to 3.3 Å resolution. It shows mostly helical structure and resembles the structure of avian farnesyl diphosphate synthase, but with the addition of two loop regions.

1. Introduction

Farnesyl diphosphate synthase (FPPS) catalyses the formation of farnesyl diphosphate (FPP) from dimethylallyl diphosphate (DMAPP) and isopentenyl diphosphate (IPP) (van Beek *et al.*, 1999; Keller & Fliesler, 1999; Grove *et al.*, 2000; Dunford *et al.*, 2001) and is inhibited by the bisphosphonate class of drugs used in bone-resorption therapy (Rodan & Reszka, 2002; Geusens & McClung, 2001; Pistevou-Gombaki *et al.*, 2002). Such bisphosphonates have also recently been shown to have potent activity as anti-parasitic agents, especially against diseases caused by the trypanosomatid parasites *Leishmania mexicana*, *L. donovani*, *Trypanosoma cruzi* and *T. brucei*, the causative agents of cutaneous and visceral leishmaniasis, Chagas' disease and sleeping sickness, respectively (Martin *et al.*, 2001; Yardley *et al.*, 2002; Rodriguez *et al.*, 2002; Ghosh *et al.*, 2004). In *T. brucei*, FPPS has been validated as a drug target by using RNA-interference techniques (Montalvetti *et al.*, 2003). FPPS inhibition by bisphosphonates is also of interest since these molecules stimulate $\gamma\delta$ T cells of the human immune system, resulting in both antibacterial and anti-cancer activity (Das *et al.*, 2001; Miyagawa *et al.*, 2001; Sanders *et al.*, 2004; Kunzmann *et al.*, 2000; Wilhelm *et al.*, 2003). A recent study (Hosfield *et al.*, 2004) reported the crystallographic structure of a prokaryotic FPPS bound to a bisphosphonate plus IPP and in earlier work (Tarshis *et al.*, 1996) the structure of a eukaryotic (avian) FPPS was reported in the absence or presence of isoprenoid diphosphates. Here, we report our progress in determining the structure of FPPS from *T. brucei*, an organism which causes over 300 000 cases of African sleeping sickness annually and for which there are no good treatments. We have expressed and purified *T. brucei* FPPS (390 amino acids, MW = 44.4 kDa) and obtained FPPS single crystals both in the absence and presence of the potent bisphosphonate inhibitor minodronate, together with a 3.3 Å resolution structure of FPPS crystallized in the absence of minodronate obtained using the molecular-replacement method.

2. Materials and methods

2.1. Protein preparation

The *T. brucei* FPPS gene, which encodes 367 amino-acid residues, was amplified by the polymerase chain reaction (PCR) and inserted into the vector pET-28a$^+$ (Novagen) to give pETFPPS (Montalvetti *et al.*, 2003). 23 extra residues, including a six-His tag, were added to the N-terminal position. The recombinant plasmid was then transformed into the host *Escherichia coli* BL21(DE3) for expression. Bacterial clones were grown in LB medium containing 25 µg ml^{-1} kanamycin. To perform induction, the bacterial cells were first grown to an A_{600} of 0.4–0.6 at 310 K and 1 m*M* isopropyl-β-D-thiogalactoside was then added. After 5 h growth at 310 K, cells were pelleted by centrifugation, washed with Dulbecco's phosphate-buffered saline (Pierce) and resus-

pended in B-per bacterial protein-extraction reagent (Pierce), incubated with 10 mg ml^{-1} lysozyme and 10 µl ml^{-1} protease-inhibitor cocktail (Sigma) for 15 min on ice, incubated with 1 µl ml^{-1} Benzonase nuclease (Novagen) for 15 min on ice and then centrifuged at 15 000*g* for 15 min at 277 K.

The supernatant was loaded onto a pre-equilibrated Ni–NTA FPLC column and washed with binding buffer (500 m*M* NaCl, 20 m*M* Na_2HPO_4 pH 7.4). Protein was eluted from the column with the same buffer but containing 500 m*M* imidazole. The eluted fraction was concentrated by ultrafiltration using an Amicon cell (Millipore), desalted with a PD-10 desalting column (Amersham Biosciences) and stored in 10 m*M* HEPES buffer pH 7.4 containing 10 m*M* 2-mercaptoethanol. Protein purity was determined by mass spectrometry and by SDS–PAGE and was found to be >95% homogeneous. Protein concentration was determined by the method of Bradford (1976), using bovine serum albumin as the standard. Enzyme activity was determined using the radiometric assay described previously (Montalvetti *et al.*, 2001) in the presence of either 10%(*w*/*v*) polyethylene glycol (PEG) 8000, 5%(*w*/*v*) PEG 8000, 10%(*v*/*v*) PEG 600 or 10%(*v*/*v*) glycerol in order to test their effects on enzyme activity. The optimal conditions for maintaining enzyme activity on storage were found to be use of HEPES buffer with 10%(*w*/*v*) PEG 8000 at 193 K.

2.2. Crystallization

Initial crystallization screening was performed based on sparse-matrix (Jancarik & Kim, 1991) conditions using Hampton Research (Laguna Niguel, CA, USA) Crystal Screens with the hanging-drop vapour-diffusion method. In general, 1 µl of solution [10 m*M* HEPES, 10 m*M* 2-mercaptoethanol, 10%(*w*/*v*) PEG 8000 pH 7.4] containing *T. brucei* FPPS (5–20 mg ml^{-1}) was mixed with 1 µl reservoir solution and the mixture was incubated at 277 K. Small FPPS crystals were observed under a variety of conditions; for example, 0.2 *M* potassium citrate monohydrate with 20%(*w*/*v*) PEG 3350 pH 8.3 or 0.1 *M* HEPES with 10%(*w*/*v*) PEG 8000 and 8%(*v*/*v*) ethylene glycol pH 7.5. The effects of protein concentration, precipitant concentration, buffer type, buffer pH value and metal-ion concentration were then optimized and we finally obtained protein crystals that gave good diffraction patterns. Typical conditions were 10 mg ml^{-1} FPPS in 0.1 *M* sodium cacodylate and 0.2 *M* magnesium acetate tetrahydrate with 20%(*w*/*v*) PEG 8000 pH 6.5. To attempt growth of the drug-bound protein crystals, we mixed FPPS with minodronate at a ratio of 1:5 and incubated the mixture overnight. Crystallization experiments were then carried out and good single crystals were obtained from a 10 mg ml^{-1} minodronate/FPPS solution containing 100 m*M* ammonium acetate, 20%(*v*/*v*) 1,2-propanediol and 0.5 m*M* magnesium chloride pH 5.75. Prior to data collection at 100 K, crystals were mounted in a cryoloop and flash-frozen in liquid nitrogen after addition of 40%(*w*/*v*) sucrose or 40%(*v*/*v*) PEG 400 as cryoprotectant.

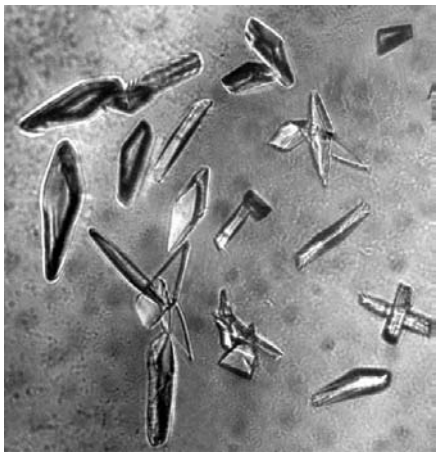

Figure 1
Crystals of farnesyl diphosphate synthase (FPPS) from *T. brucei*. The largest crystals are ~0.3 × 0.1 × 0.05 mm.

2.3. Data collection and analysis

Preliminary X-ray diffraction experiments were carried out by using a Bruker general area-detector diffraction system. Higher resolution X-ray data were then collected using synchrotron radiation and an ADSC Q315 CCD detector at Brookhaven National Synchrotron Light Source beamline X12B (wavelength λ = 1.1 Å). Crystallographic data were processed using the *HKL*2000 program package (Otwinowski & Minor, 1997). An initial model was built using *CCP*4 (Collaborative Computational Project, Number, 1994) and *O* (Jones *et al.*, 1991). This model was then improved by manually rebuilding it using *O* (Jones *et al.*, 1991) and was finally refined using *X-PLOR* (Brünger, 1992).

3. Results and discussion

Under the crystallization conditions described above, single crystals appeared between days 4 and 7 and grew to maximum dimensions of 0.3 × 0.1 × 0.05 mm after 30 d at 277 K. Fig. 1 shows a typical photograph of a collection of such crystals for FPPS in the absence of minodronate. The crystals belong to the *I*-centred orthorhombic space group *I*222, with unit-cell parameters $a = 61.43$, $b = 118.12$, $c = 120.04$ Å. Assuming the presence of one molecule per asymmetric unit, the Matthews coefficient V_M (Matthews, 1968) is 2.65 Å^3 Da^{-1}, giving a solvent content of 54%. Crystals of FPPS obtained in the presence of minodronate belong to the *C*-centred monoclinic space group *C*2, with unit-cell parameters $a = 131.98$, $b = 118.10$, $c = 63.25$ Å, $\beta = 112.48^\circ$. Assuming the presence of two molecules per asymmetric unit, the Matthews coefficient V_M (Matthews, 1968) is 2.77 Å^3 Da^{-1}, giving a solvent content of

Table 1
Data-collection statistics for *T. brucei* FPPS crystals grown in the absence and presence of minodronate.

Values in parentheses are for the highest resolution shell.

	FPPS†	FPPS (minodronate)‡
Space group	*I*222	*C*2
Unit-cell parameters		
a (Å)	61.43	131.98
b (Å)	118.12	118.10
c (Å)	120.04	63.25
α (°)	90	90
β (°)	90	112.48
γ (°)	90	90
Resolution (Å)	30–3.30 (3.42–3.30)	30–2.50 (2.59–2.50)
Total reflections	11249	58216
Unique reflections	6202	30546
Completeness (%)	90.4 (56.2)	96.5 (79.4)
R_{merge} (%)	14.3 (28.6)	6.9 (35.6)
Average $I/\sigma(I)$	24.6 (5.4)	28.2 (3.3)
Multiplicity	9.3	3.4

† FPPS crystals grown in the absence of minodronate. ‡ FPPS crystals grown in the presence of minodronate.

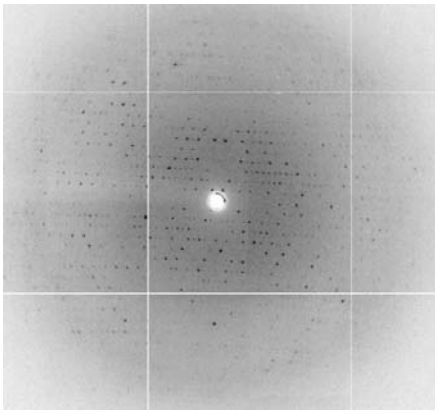

Figure 2
X-ray diffraction pattern for FPPS crystals grown in the presence of minodronate obtained using synchrotron radiation at Brookhaven National Synchrotron Light Source beamline X12B.

Figure 3
Comparison of the amino-acid sequences of avian FPPS and *T. brucei* FPPS. The numbers are for the *T. brucei* sequence. Identical amino-acid residues are shaded green. The red boxes indicate insertions found in *T. brucei* and contribute to the loops shown in Fig. 4.

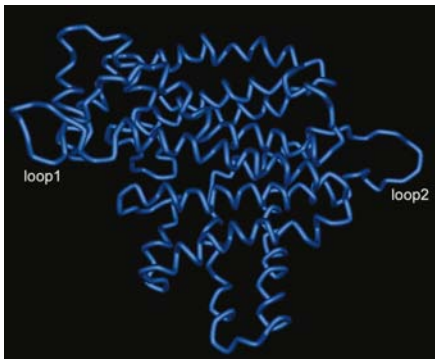

Figure 4
The α-carbon tracing of the *T. brucei* FPPS crystal structure, showing loops 1 and 2 (Fig. 3).

55%. Fig. 2 shows the X-ray diffraction pattern from such a crystal obtained using synchrotron radiation; data-collection statistics for both types of crystal are shown in Table 1.

Since there is only one molecule in the asymmetric unit, we have begun to analyze the structure of FPPS crystallized in the absence of minodronate. Molecular replacement using the avian FPPS (Tarshis *et al.*, 1996) as a model (PDB code 1ubv) did not yield a satisfactory solution, perhaps in part owing to the low (35%) sequence identity (Fig. 3). We therefore next used the homology model of the *T. brucei* FPPS reported previously (Montalvetti *et al.*, 2003) (which was derived from the avian structure using *Insight*II 2000.1) as a template and found a good solution with an R value of 0.45. We carried out rigid-body fitting, positional refinement by simulated annealing and B-factor refinement using *X-PLOR* (Brünger, 1992). The resulting difference electron density ($2F_o - F_c$) maps were used to place water molecules in the structure and to manually reposition side-chain atoms in the protein using the *O* program (Jones *et al.*, 1991). This process of adding water, model rebuilding and refinement was repeated until no 2σ or greater difference electron density was observed. The R and R_{free} values found were 0.23 and 0.31, respectively, for all of the 3.3 Å resolution data. The overall protein structure found is similar to that seen in the avian FPPS, except that there are two insertion loops (residues 65–74 and 184–194) in the *T. brucei* structure, as shown in Fig. 4. For the higher resolution data set, we again attempted the molecular-replacement method using the refined FPPS monomer structure as a template and obtained two pairs of reasonably good solutions. For the first, R = 50.9%, Corr-F = 42.3, Corr-I = 50.7; for the second, R = 55.5%, Corr-F = 32.4, Corr-I = 37.9. The initial electron-density maps clearly show that there are two molecules in the asymmetric unit and that the protein is mainly composed of α-helices. Further structure refinement is still in progress.

In summary, we have crystallized the FPPS enzyme from *T. brucei* and obtained diffraction data at 3.3 Å for the drug-free protein and at 2.5 Å for a second form crystallized in the presence of the bisphosphonate drug minodronate. Using a homology model, we have obtained a structure of the orthorhombic form (having R = 0.23 and R_{free} = 0.31) which is similar to that seen in the avian enzyme, but with the addition of two loop regions.

This work was supported by the United States Public Health Service (National Institutes of Health Grant GM-65307) and was carried out in part at the National Synchrotron Light Source, Brookhaven National Laboratory, which is supported by the US Department of Energy, Division of Materials Sciences and Division of Chemical Sciences under Contract No. DE-AC02-98CH10886 and by NIH NCRR. JM was supported by an American Heart Association, Midwest Affiliate Predoctoral Fellowship (grant 0315261Z).

References

Beek, E. van, Pieterman, E., Cohen, L., Löwik, C. & Papapoulos, S. (1999). *Biochem. Biophys. Res. Commun.* **264**, 108–111.
Bradford, M. M. (1976). *Anal. Biochem.* **72**, 248–254.
Brünger, A. T. (1992). *X-PLOR, Version 3.1*. New Haven, CT, USA: Yale University Press.
Collaborative Computational Project, Number 4 (1994). *Acta Cryst.* D**50**, 760–763.
Das, H., Wang, L., Kamath, A. & Bukowski, J. F. (2001). *Blood*, **98**, 1616–1618.
Dunford, J. E., Thompson, K., Coxon, F. P., Luckman, S. P., Hahn, F. M., Poulter, C. D., Ebetino, F. H. & Rogers, M. J. (2001). *J. Pharmacol. Exp. Ther.* **296**, 235–242.
Geusens, P. & McClung, M. (2001). *Exp. Opin. Pharmacother.* **2**, 2011–2025.
Ghosh, S., Chan, J. M., Lea, C. R., Meints, G. A., Lewis, J. C., Tovian, Z. S., Flessner, R. M., Loftus, T. C., Bruchhaus, I., Kendrick H., Croft, S. L., Kemp, R. G., Kobayashi, S., Nozaki, T. & Oldfield, E. (2004). *J. Med. Chem.* **47**, 175–187.
Grove, J. E., Brown, R. J. & Watts, D. J. (2000). *J. Bone Miner. Res.* **15**, 971–981.
Hosfield, D. J., Zhang, Y., Dougan, D. R., Broun, A., Tari, L. W., Swanson, R. V. & Finn, J. (2004). *J. Biol. Chem.* **279**, 8526–8529.
Jancarik, J. & Kim, S.-H. (1991). *J. Appl. Cryst.* **24**, 409–411.
Jones, T. A., Zou, J. Y., Cowan, S. W. & Kjeldgaard, M. (1991). *Acta Cryst.* A**47**, 110–119.
Keller, R. K. & Fliesler, S. J. (1999). *Biochem. Biophys. Res. Commun.* **266**, 560–563.
Kunzmann, V., Bauer, E., Feurle, J., Weissinger, F., Tony, H. P. & Wilhelm, M. (2000). *Blood*, **96**, 384–392.
Martin, M. B., Grimley, J. S., Lewis, J. C., Heath, H. T. III, Bailey, B. N., Kendrick, H., Yardley, V., Caldera, A., Lira, R., Urbina, J. A., Moreno, S. N., Docampo, R., Croft, S. L. & Oldfield, E. (2001). *J. Med. Chem.* **44**, 909–916.
Matthews, B. W. (1968). *J. Mol. Biol.* **33**, 491–497.
Miyagawa, F., Tanaka, Y., Yamashita, S. & Minato, N. (2001). *J. Immunol.* **166**, 5508–5514.
Montalvetti, A., Bailey, B. N., Martin, M. B., Severin, G. W. E., Oldfield, E. & Docampo, R. (2001). *J. Biol. Chem.* **276**, 33930–33937.
Montalvetti, A., Fernandez, A., Sanders, J. M., Ghosh, S., van Brussel, E., Oldfield, E. & Docampo, R. (2003). *J. Biol. Chem.* **278**, 17075–17083.
Otwinowski, Z. & Minor, W. (1997). *Methods Enzymol.* **276**, 307–326.
Pistevou-Gombaki, K., Eleftheriadis, N., Sofroniadis, I., Makris, P. & Kouloulias, V. (2002). *J. Exp. Clin. Cancer Res.* **21**, 429–432.
Rodan, G. A. & Reszka, A. A. (2002). *Curr. Mol. Med.* **2**, 571–577.
Rodriguez, N., Bailey, B. N., Martin, M. B., Oldfield, E., Urbina, J. A. & Docampo, R. (2002). *J. Infect. Dis.* **186**, 138–140.

Sanders, J. M., Ghosh, S., Chan, J. M., Meints, G., Wang, H., Raker, A. M., Song, Y., Colantino, A., Burzynska, A., Kafarski, P., Morita, C. T. & Oldfield, E. (2004). *J. Med. Chem.* **47**, 375–384.

Tarshis, L. C., Proteau, P. J., Kellogg, B. A., Sacchettini, J. C. & Poulter, C. D. (1996). *Proc. Natl Acad. Sci. USA*, **93**, 15018–15023.

Wilhelm, M., Kunzmann, V., Eckstein, S., Reimer, P., Weissinger, F., Ruediger, T. & Tony, H. P. (2003). *Blood*, **102**, 200–206.

Yardley, V., Khan, A. A., Martin, M. B., Slifer, T. R., Araujo, F. G., Moreno, S. N., Docampo, R., Croft, S. L. & Oldfield, E. (2002). *Antimicrob. Agents Chemother.* **46**, 929–931.